Electrochemical and Solid-State Letters, **14** (10) A157-A160 (2011)
1099-0062/2011/14(10)/A157/4/$28.00 © The Electrochemical Society

Development of an Ordered Mesoporous Carbon/MoO_2 Nanocomposite for High Performance Supercapacitor Electrode

Yuanyuan Zhou, Chul Wee Lee, and Songhun Yoon[*,z]

Green Chemical Technology Division, Korea Research Institute of Chemical Technology and University of Science and Technology, Daejeon 305-600, Korea

An ordered mesoporous nanocomoposite of carbon-MoO_2 was prepared by incorporation of Mo precursor into mesopores of ordered mesoporous carbon after acid treatment. In spite of crystal growth, inner mesopores of the carbon were covered by MoO_2, which was attributed to strong interaction between the Mo precursor and the acidified carbon surface. When applied into supercapacitor electrode, an improved volumetric capacitance (216 F cm^{-3}) and a very high pseudocapacitance by MoO_2 itself (622 F g^{-1}) were obtained, indicative of an efficient capacitive utilization of MoO_2 within carbon mesopores. Because of the characteristic nanostructure, furthermore, rate capability and cycle performance were improved.
 [DOI: 10.1149/1.3614517]

Manuscript submitted May 26, 2011; revised manuscript received June 16, 2011. Published July 27, 2011.

Recently, the supercapacitors (SCs) have been investigated as high power energy sources for use in digital communications, hybrid electric vehicles (HEVs), and EVs.[1–5] Since pseudocapacitors utilize charges accumulated during a Faradaic reaction, they exhibit a higher capacitance than electric double-layer capacitors (EDLCs). In general, various transition metal (Ru, Mn, Fe, V, W, Co, and Ni) oxide materials have been employed as pseudocapacitor electrodes.[6–13] Nanostructure of such metal oxides has been investigated due to its high surface area for charge storage, the better electrolyte transport within mesopores and the short proton diffusion path, which can result in a better rate capability.[7,13] As novel pseudocapacitor electrode materials, molybdenum oxides (MoO_3 and MoO_2) have been investigated and various forms of nanorod, nanowire and nanocomposite with activated carbon or conducting polymer have been prepared.[14–20] Since the improved rate capability has been observed for the ordered mesoporous carbon (OMC) ELDC electrodes, the high rate capability and the large capacitance are expected in the nanocomposite between MoO_2 and OMC, which has been not tried yet.[21,22] Especially, OMC material prepared by the tri-constituent co-assembly (TCCA) method using silicate, surfactant and carbon precursor exhibited a bimodal mesoporous structure with abundant small mesopores within the nanosized carbon walls, which can give additional sites for an incorporation of pseudocapacitive metal oxide.[23]

Herein, an ordered mesoporous nanocomposite of carbon-MoO_2 is prepared by a post-addition of Mo precursor into the mesopores of OMC obtained from TCCA method. For the purpose of a high interaction between Mo precursor and inner surface of carbon, an acid treatment of OMC is conducted. After an incorporation of Mo precursor into the mesopores and a following calcination, the nanocomposite material is prepared. Structure and morphology of the prepared materials are analyzed. Supercapacitor performance is investigated after fabrication of electrodes using the prepared materials.

Experimental

An ordered mesoporous carbon was prepared by TCCA method using resol, silicate and F127 block copolymer, which was reported in the literatures.[24,25] So the prepared carbon material was named tri-constituent ordered mesoporous carbon (tOMC). With this tOMC material, an ordered mesoporous carbon-MoO_2 composite (tOMC-MO) was prepared using a simple two-step method. Typically, tOMC powders which were prepared by the employed method were immersed in 20 wt % HNO_3 solution at 70°C for 24 h for the purpose of surface acidification.[26] After drying, 0.11 g of acidified tOMC was vacuumed and immersed into 15.0 g of phosphomolybdic acid (PMA) ethanolic solution (containing 0.6 g of PMA) under stirring. The powders collected after filtration were washed using ethanol twice and dried at 100°C. Sequentially the powers were calcined at 700°C for 2 h in an 4 mol % H_2/N_2 mixed atmosphere. After cooling down to the room temperature, tOMC-MO material was obtained. The pore size distribution (PSD) was analyzed using an N_2 adsorption measurement (Micromeritics ASAP 2010). The external morphology of the carbon was examined using a scanning electron microscope (SEM, JEOL JSM-840A), whereas the pore image was scanned by a transmission electron microscope (TEM, JEOL JEM-2010). The X-ray diffraction patterns were obtained with a Rigaku D/Max-3C diffractometer equipped with a rotating anode and Cu K_α radiation ($\lambda = 0.15418$ nm).

The electrode fabrication procedure and electrochemical cell structure were identical with the reported literature.[4,5,8,13] Here, Pt flag counter and SCE reference electrodes were used for three electrode cell system using 1.0 M H_2SO_4 electrolyte. Ivium potentiostat was utilized to conduct cyclic voltametry (CV) and electrochemical impedance spectroscopy (EIS). Scan rate was varied from 2 to 50 mV s^{-1} in CV experiment. For EIS measurement, sinusoidal voltage of 10 mV amplitude was applied in the frequency range used was 10^6 Hz–5 mHz. Galvanostatic charge-discharge experiment was carried out using WBCS-3000 battery cycler (Xeno Co.).

Results and Discussion

Figure 1 displays the small angle and wide angle x-ray diffraction (XRD) patterns of the prepared materials. In tOMC material, a sharp peak was observed at $2\theta = 1.0°$ and a shoulder appeared near 1.5°, which were associated with a highly ordered (2D hexagonal) mesoporous structure.[24,25] For tOMC-MO material, however, the ordered structure was maintained in spite of a decrease of peak intensity, which was attributed to the formation of MoO_2 crystals within pores and a partial collapse of ordered structure. From a wide angle XRD pattern in Fig. 1b, it was shown that tOMC-MO showed the characteristic peaks of monoclinic MoO_2 [JCPDS no. 76-1807] and average 9 nm MoO_2 crystals were estimated by Sherrer's Equation.[27] From ICP analysis, weight fraction of carbon (x_{carbon}) and MoO_2 (x_{MoO_2}) were 73 and 27 wt %, respectively.

In Figs. 2a and 2b, the nitrogen sorption isotherms and the pore size distributions (PSDs) were shown. Here, the pore volume of tOMC-MO decreased while the sorption isotherms remained similar. A monodispersed PSD was obtained in tOMC-MO with a size of 3.94 nm, but tOMC showed a bimodal PSD with sizes of 4.28 and 2.64 nm, which corresponded to the hydrophobic part in the F127 surfactant micelle and the occupied sites of the silica, respectively.[24,25] As shown in Fig. 2b, the small pores completely disappeared and a slight decrease of large pore size from 4.28 to 3.94 nm was observed in tOMC-MO, which indicated that MoO_2 occupied the small pores completely and the inner mesopores were partially covered by MoO_2. Measured surface areas of tOMC and tOMC-MO

* Electrochemical Society Active Member.
z E-mail: yoonshun@krict.re.kr

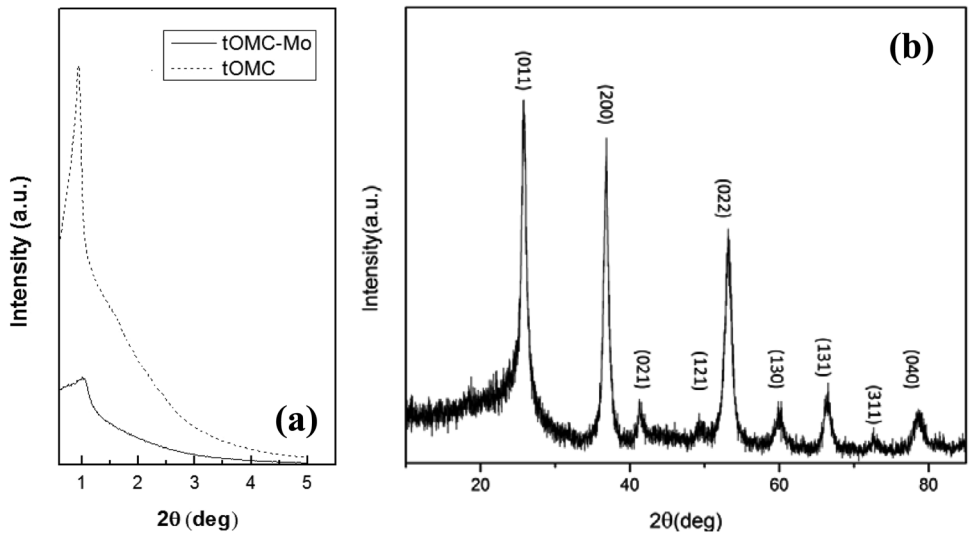

Figure 1. (a); Small angle x-ray scattering patterns for tOMC and tOMC-Mo materials. (b); Wide angle x-ray diffraction patterns for OMC-Mo.

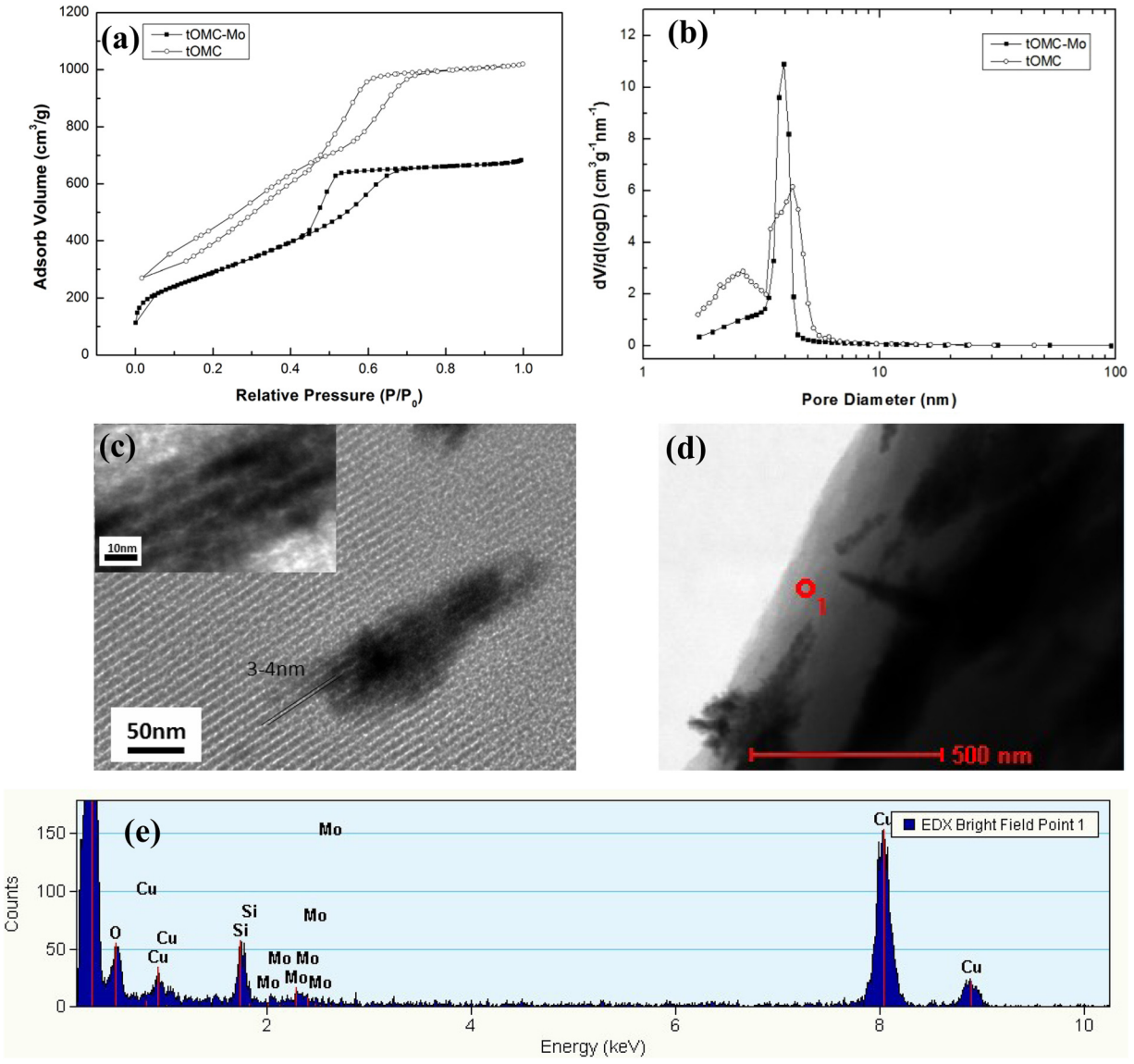

Figure 2. (Color online) Nitrogen sorption isotherms (a) and BJH pore size distributions (b) of tOMC (hollow circle) and tOMC-Mo (solid rectangle). (c), (d) and (e) are TEM, HRTEM and STEM images of tOMC-Mo respectively and its elemental analysis using EDX spot in (d) image.

were 1639 and 1052 $m^2\ g^{-1}$, respectively. In addition, the pore volume of OMC (1.577 g cm^{-3}) was reduced to 1.056 g cm^{-3} of tOMC-MO material. Also, theoretical density of tOMC and tOMC-MO were 0.476 and 0.669 g cm^{-3}, respectively, which was calculated using the pore volume values and the density of carbon (1.9 g cm^{-3}) and MoO_2 (4.7 g cm^{-3}).

TEM analysis was conducted in order to investigate pore structure and position of MoO_2 crystals. As shown in Figs. 2c and 2d, TEM images of tOMC-MO revealed that the ordered mesopores was maintained while aggregated MoO_2 crystals were observed, which was probably due to the high calcination temperature (700°C). From an inset in Fig. 2c, it was observed that smaller ordered mesopores existed even within the aggregated MoO_2 crystals. The elemental analysis using EDX point mode was conducted for a red spot in Fig. 2d and its result was displayed in Fig. 2e. Clearly, Mo element was observed, which demonstrated that MoO_2 occupied the inner surface of carbon mesopores in tOMC, which coincided with the pore size change from 4.28 to 3.94 nm in Fig. 2b.

In Fig. 3, cyclic voltamograms for tOMC and tOMC-MO electrodes were shown. For tOMC electrode, the rectangular shape characteristic to EDLC was observed ($\sim$100 F g^{-1} in anodic scan). As for tOMC-MO electrode, however, three redox peaks associated with the pseudocapcitive reactions of MoO_2 were observed. These peaks were probably associated with the change of oxidation state of Mo metal, which requires a further investigation.[14] From the literatures, an increase of capacitance with the overall shape maintained was reported when the composite with MoO_2 or MoO_3 were prepared.[16,20] In our tOMC-MO electrode, interestingly, three pseudocapacitive redox peaks were distinctly observed and total capacitance in tOMC-Mo electrode largely increased. Note that peak capacitance (C_{peak}) at 0.105 V *vs*. SCE was 322 F g^{-1}, which is much higher than the double layer capacitance of tOMC electrode ($C_{tOMC} = 154$ F g^{-1}). From simple calculation, pseudocapacitive fraction by MoO_2 itself (C_{MoO_2}) was as high as about 622 F g^{-1} [$(C_{MoO_2}) = (C_{peak} - C_{OMC})/x_{MoO_2}$), which was certainly attributed to the high dispersion of MoO_2 within mesopores of carbon as shown in Fig. 2. Furthermore, a high volumetric capacitance (216 F cm^{-3}) of tOMC-MO electrode was observed but tOMC electrode showed only 73 F cm^{-3}, which was due to the density increase in tOMC-MO. Figure 3b exhibited a change of cyclic voltamogram as a scan rate increased. According to increase of scan rate, collapse of the pseudocapacitive peaks appeared but double layer capacitance remained less varied, indicative of a high rate capability relevant to the fast electrolyte transport within the ordered mesopores in tOMC-MO, which was also confirmed by a preliminary EIS experiments (not shown here). Only slight increase of resistance was observed in tOMC-MO electrode, which was attributed to the high mesoporosity even after MoO_2 incorporation as shown in Fig. 2b. Hence, the mesopores of tOMC-MO remained utilized for charge storage in the electric double-layer while the pseudocapacitive sites became

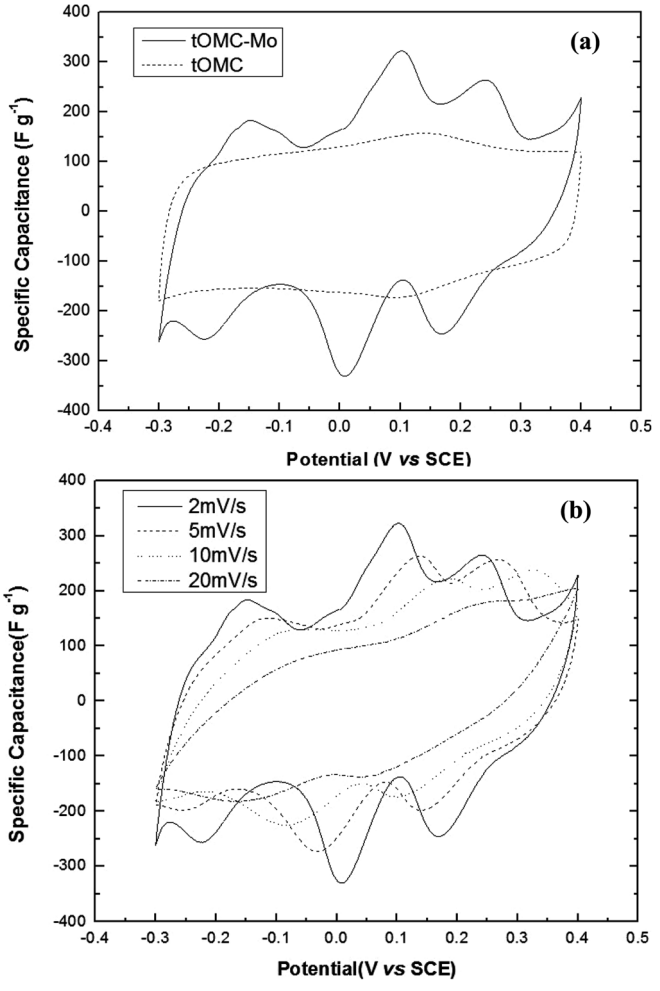

Figure 3. (a); Capacitance vs. potential profiles of tOMC (dot line) and tOMC-Mo (solid line), which was obtained by dividing current in CV experiment with scan rate (2 mV s^{-1}). (b); Scan rate dependency of tOMC-Mo electrode with 2 (solid line), 5 (dash line), 10 (dot line), 20 mV s^{-1} (dash-dot line).

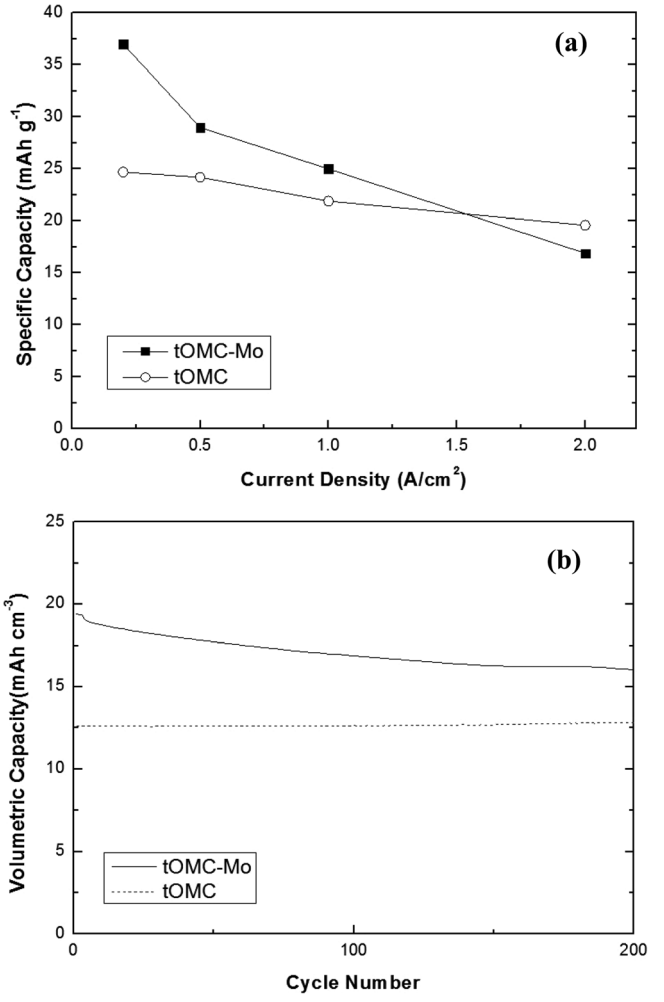

Figure 4. (a); Specific capacity vs. current density of tOMC-Mo electrode with an increasing current. The applied currents were indicated within the figure. (b); Cycle performance of tOMC-Mo (solid line) and tOMC electrode (dot line) until 200 cycles.

unavailable according to an increase of scan rate as shown in Fig. 3b.

In Fig. 4a, the rate capability comparison was plotted. At low current density, tOMC-MO exhibited a much higher capacity due to its higher pseudocapacitive charging at MoO_2. As the current density increased, a gradual decrease of capacity was observed in tOMC-MO electrode while tOMC electrode showed an invariant capacity due to its EDLC charging mechanism.[22,25] Note that tOMC-MO electrode exhibited a high capacity even under very high current density of 1.0 A cm^{-2}, indicative of an excellent rate capability of tOMC-MO electrode. Figure 4b shows cycle performance of tOMC and tOMC-MO electrodes until 200 cycles. It was reported that capacitance retention about 86% was observed for MoO_2 nanorod electrode after 50 cycles using 1 M H_2SO_4 electrolyte.[14] As for tOMC-MO electrode, an improved cycle performance was observed ($\sim$90% retention at 50 cycles), which was probably relevant to a hindered exposal of MoO_2 to electrolyte than the nanorod electrode.[21]

Conclusion

Because of uniform incorporation of MoO_2 into mesopores, tOMC-MO electrode exhibited a higher specific, a volumetric capacitance, a high rate capability and an improved cycle performance, which were attributed to a complete nanocomposite formation and a uniform coverage of MoO_2 within inner pores of carbon.

Acknowledgment

This research was supported by the project of Korea Research Institute of Chemical Technology (KRICT).

References

1. C. Liu, Z. Yu, D. Neff, A. Zhamu, and B. Z. Jang, *Nano Lett.*, **10**, 4863 (2010).
2. B. E. Conway, *Electrochemical Supercapacitors*, Kluwer Academic/Plenum, New York (1999).
3. L. L. Zhang and X. S. Zhao, *Chem. Soc. Rev.*, **38**, 2520 (2009).
4. S. Yoon, S. M. Oh, C. W. Lee, and J. H. Ryu, *J. Electroanal. Chem.*, **650**, 187 (2011).
5. S. Yoon, J. Lee, T. Hyeon, and S. M. Oh, *J. Electrochem. Soc.*, **147**, 2507 (2000).
6. D. Kalpana, K. S. Omkumar, S. S. Kumar, and N. G. Renganathan, *Electrochim. Acta*, **52**, 1309 (2006).
7. L. L. Zhang, T. Wei, W. Wang, and X. S. Zhao, *Microporous Mesoporous Mater.*, **123**, 260 (2009).
8. S. Yoon, S. M. Oh, and C. Lee, *Mater. Res. Bull.*, **44**, 1663 (2009).
9. V. Srinivasan and J. W. Weidner, *J. Electrochem. Soc.*, **144**, L220 (1997).
10. V. R. Shinde, S. B. Mahadik, T. P. Gujar, and C. D. Lokhande, *Appl. Surf. Sci.*, **252**, 7487 (2006).
11. S. Y. Wang, K. C. Ho, S. L. Kuo, and N. L. Wu, *J. Electrochem. Soc.*, **153**, A75 (2006).
12. R. N. Reddy and R. G. Reddy, *J. Power Sources*, **156**, 700 (2006).
13. S. Yoon, E. Kang, J. K. Kim, C. W. Lee, and J. Lee, *Chem. Commun.*, **47**, 1021 (2011).
14. J. Rajeswari, P. S. Kishore, B. Viswanathan, and T. K. Varadarajan, *Electrochem. Commun.*, **11**, 572 (2009).
15. V. Murugan, A. K. Viswanath, C. S. Gopinath, and K. Vijayamohanan, *J. Appl. Phys.*, **100**, 074319 (2006).
16. W. Sugimoto, T. Ohnuma, Y. Murakami, and Y. Takasu, *Electrochem. Solid-State Lett.*, **4**, A145 (2001).
17. Y. Takasu, T. Ohnuma, W. Sugimoto, and Y. Murakami, *Electrochemistry*, **67**, 1187 (1999).
18. A. V. Murugan, A. K. Viswanath, G. Campet, C. S. Gopinath, and K. Vijayamohanan, *Appl. Phys. Lett.*, **87**, 243511 (2005).
19. B. Qi, X. Ni, D. Li, and H. Zheng, *Chem. Lett.*, **37**, 336 (2008).
20. F. Gao, L. Zhang, and S. Huang, *Mater. Lett.*, **64**, 537 (2010).
21. H.-Q. Li, R.-L. Liu, D.-Y. Zhao, and Y.-Y. Xia, *Carbon*, **45**, 2628 (2007).
22. V.-G. Cathie, E. Frackowiak, K. Jurewicz, M. Friebe, J. Parmentier, and F. Béguin, *Carbon*, **43**, 1293 (2005).
23. Y.-Q. Dou, Y. Zhai, H. Liu, Y. Xia, B. Tu, D. Zhao, and X.-X. Liu, *J. Power Sources*, **196**, 1608 (2011).
24. Y. Zhou, Y. Kim, C. Jo, J. Lee, C. W. Lee, and S. Yoon, *Chem. Commun.*, **47**, 4944 (2011).
25. R. Liu, Y. Shi, Y. Wan, Y. Meng, F. Zhang, D. Gu, Z. Chen, B. Tu, and D. Zhao, *J. Am. Chem. Soc.*, **128**, 11652 (2006).
26. X. Ji, K. T. Lee, and L. F. Nazar, *Nature Mater.*, **8**, 500 (2009).
27. A. L. Patterson, *Phys. Rev.*, **56**, 978 (1939).